

Graph Signal Diffusion Model for Collaborative Filtering

Yunqin Zhu

University of Science and Technology of China
School of Information Science and Technology
Hefei, China
haaasined@gmail.com

Qi Zhang

Shanghai AI Laboratory
Shanghai, China
zhangqi.fqz@gmail.com

Chao Wang*

Guangzhou HKUST Fok Ying Tung Research Institute
Guangzhou, China
University of Science and Technology of China
School of Computer Science and Technology
Hefei, China
chadwang2012@gmail.com

Hui Xiong*

The Hong Kong University of Science and Technology
(Guangzhou), Thrust of Artificial Intelligence
Guangzhou, China
The Hong Kong University of Science and Technology
Department of Computer Science and Engineering
Hong Kong SAR, China
xionghui@ust.hk

ABSTRACT

Collaborative filtering is a critical technique in recommender systems. It has been increasingly viewed as a conditional generative task for user feedback data, where newly developed diffusion model shows great potential. However, existing studies on diffusion model lack effective solutions for modeling implicit feedback. Particularly, the standard isotropic diffusion process overlooks correlation between items, misaligned with the graphical structure of the interaction space. Meanwhile, Gaussian noise destroys personalized information in a user’s interaction vector, causing difficulty in its reconstruction. In this paper, we adapt standard diffusion model and propose a novel *Graph Signal Diffusion Model for Collaborative Filtering* (named GiffCF). To better represent the correlated distribution of user-item interactions, we define a generalized diffusion process using heat equation on the item-item similarity graph. Our forward process smooths interaction signals with an advanced family of graph filters, introducing the graph adjacency as beneficial prior knowledge for recommendation. Our reverse process iteratively refines and sharpens latent signals in a noise-free manner, where the updates are conditioned on the user’s history and computed from a carefully designed two-stage denoiser, leading to high-quality reconstruction. Finally, through extensive experiments, we show that GiffCF effectively leverages the advantages of both diffusion model and graph signal processing, and achieves state-of-the-art performance on three benchmark datasets.

*Corresponding authors: Chao Wang and Hui Xiong.

Permission to make digital or hard copies of all or part of this work for personal or classroom use is granted without fee provided that copies are not made or distributed for profit or commercial advantage and that copies bear this notice and the full citation on the first page. Copyrights for components of this work owned by others than the author(s) must be honored. Abstracting with credit is permitted. To copy otherwise, or republish, to post on servers or to redistribute to lists, requires prior specific permission and/or a fee. Request permissions from [permissions@acm.org](https://www.acm.org).
SIGIR '24, July 14–18, 2024, Washington, DC, USA

© 2024 Copyright held by the owner/author(s). Publication rights licensed to ACM.
ACM ISBN 979-8-4007-0431-4/24/07...\$15.00
<https://doi.org/10.1145/3626772.3657759>

CCS CONCEPTS

• **Information systems** → **Recommender systems**.

KEYWORDS

Collaborative Filtering, Diffusion Model, Graph Signal Processing

ACM Reference Format:

Yunqin Zhu, Chao Wang, Qi Zhang, and Hui Xiong. 2024. Graph Signal Diffusion Model for Collaborative Filtering. In *Proceedings of the 47th International ACM SIGIR Conference on Research and Development in Information Retrieval (SIGIR '24)*, July 14–18, 2024, Washington, DC, USA. ACM, New York, NY, USA, 11 pages. <https://doi.org/10.1145/3626772.3657759>

1 INTRODUCTION

Collaborative filtering (CF) serves as a critical technique in recommender systems. It aims to reveal a user’s hidden preferences through all the observed user feedback [16]. Over the past few decades, researchers have designed various neural networks to mine collaborative patterns from implicit feedback, such as graph neural networks (GNNs) [9, 12, 44] and autoencoders (AEs) [21, 25, 39, 46]. Some of these methods construct pair- [28] or set-wise [40] ranking loss to learn the partial order relations behind preference scores. Another increasingly popular paradigm is to minimize the point-wise distance between a reconstructed user interaction vector and its ground truth. Related works often perform dropout on the input interactions, thereby encouraging the model to predict missing ones [46]. This paradigm essentially regards CF as an inverse problem, which requires estimating the distribution of a user’s potential interactions given its masked history. Many models have been proposed for this conditional generative task. For example, Mult-VAE [21] assumed that interaction vectors follow a multinomial distribution and used variational inference to robustly optimize for likelihood. Another line of works [4, 41, 42] incorporated adversarial training to produce more realistic interactions. More recently, DiffRec [43] treated interaction vectors as noisy latent states in DDPM [14], pioneering the application of diffusion model to recommendation.

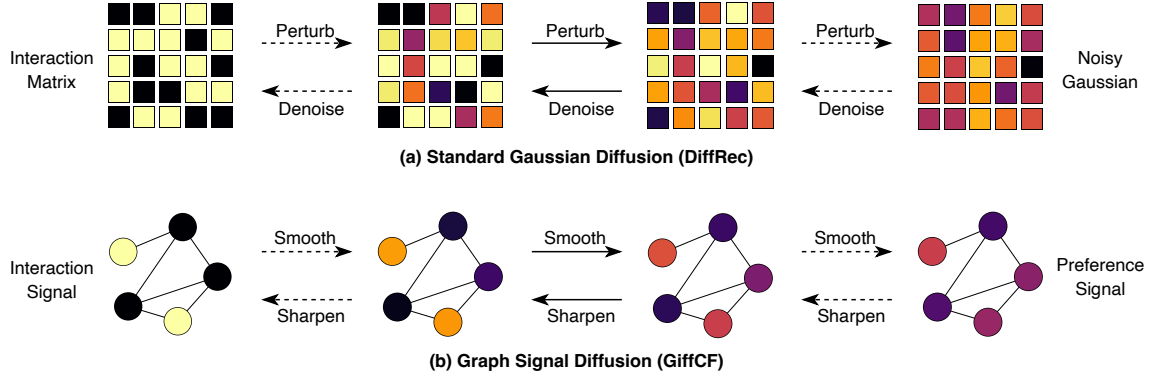


Figure 1: Comparison of different diffusion processes for implicit feedback. Standard Gaussian diffusion destroys personalized information in the interaction matrix with Gaussian noise. On the contrary, our graph signal diffusion corrupts interaction signals into smoothed preference signals, leveraging the graphical structure of the interaction space. Each square in (a) represents a matrix entry, and each circle in (b) represents a scalar-valued graph node. Deeper colors indicate higher values.

Diffusion model (DM) have made remarkable successes in solving inverse problems across multiple domains, such as image inpainting [30], speech enhancement [24], and time series imputation [36]. The ability of DM to learn complex distributions can be attributed to its hierarchical structure, which allows iterative updates of the latent states toward fine-grained directions. However, for the task of CF, the performance of standard DM is still far from satisfactory, especially when compared with the state-of-the-art graph signal processing techniques [5, 10, 33] on large datasets (see Section 4.2). We argue that standard Gaussian diffusion could have limited capabilities when modeling implicit feedback, primarily due to two reasons: (1) the isotropic diffusion process overlooks the correlation between items, leading to a misalignment with the graphical structure of the interaction space; (2) Gaussian noise destroys personalized information in user interaction vectors, causing difficulty in their reverse reconstruction. For the latter issue, Wang et al. [43] proposed to limit the variance of added noise. However, their approach still suffers from the first issue, leaving the design space of DM largely unexplored.

In this work, we adapt standard DM to address the above issues, and propose a novel *Graph Signal Diffusion Model for Collaborative Filtering* (named GiffCF). Seeing that user-item interactions are high-dimensional, sparse, yet correlated in nature, we break the routine of adding or removing Gaussian noise for distribution modeling, as image DMs usually do [14]. Instead, we view interactions as signals on the item-item similarity graph, and then define a generalized diffusion process that simulates graph heat equation (see Figure 1). Inspired by graph signal processing baselines, we design a novel family of graph smoothing filters to corrupt interaction signals in the forward process. Such forward filters introduce the graph adjacency as helpful prior knowledge for the recommendation task, overcoming the first challenge. As for high-quality reconstruction, our reverse process iteratively refines preference signals in a noise-free manner, where the update direction is conditioned on the user history and computed from a carefully designed two-stage denoiser. Through extensive experiments, we show that GiffCF effectively leverages the advantages of both DM and graph

signal processing, setting new records on three benchmark datasets. Our code is available at <https://github.com/HasiNed/GiffCF>. To summarize, our contributions are:

- (1) We propose a generalized diffusion process for CF that leverages the structure of the interaction space by smoothing and sharpening signals on the item-item similarity graph.
- (2) We unify graph signal processing baselines and propose a novel family of graph filters to smooth interaction signals in the forward process and introduce helpful inductive bias for CF.
- (3) We conduct comprehensive experiments on multiple benchmark datasets to show the superiority of our method over competitive baselines. We also provide empirical analysis of both the forward and reverse processes.

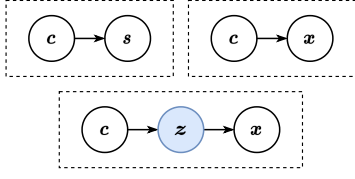
2 BACKGROUND

Conditional Gaussian diffusion. DM [14, 17, 34] has achieved state-of-the-art in many conditional generative tasks. Given an initial sample \mathbf{x} from the data distribution $q(\mathbf{x})$, the forward process of standard Gaussian diffusion is defined through an increasingly noisy sequence of latent variables deviating from \mathbf{x} , written as

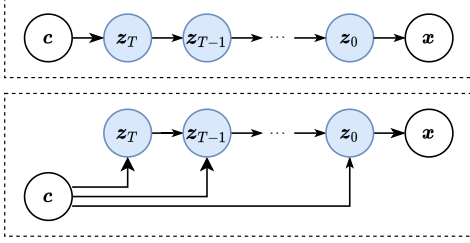
$$\begin{aligned} \mathbf{z}_t &= \alpha_t \mathbf{x} + \sigma_t \boldsymbol{\epsilon}_t, \\ \boldsymbol{\epsilon}_t &\sim \mathcal{N}(\mathbf{0}, \mathbf{I}), \quad t = 0, 1, 2, \dots, T, \end{aligned} \quad (1)$$

or $q(\mathbf{z}_t | \mathbf{x}) = \mathcal{N}(\mathbf{z}_t; \alpha_t \mathbf{x}, \sigma_t^2 \mathbf{I})$. In a variance-preserving noise schedule, the noise level σ_t monotonically increases from 0 to 1, while the signal level α_t is constrained by $\alpha_t^2 + \sigma_t^2 = 1$. To see how \mathbf{z}_s and \mathbf{z}_t from two arbitrary timesteps transition to each other, we write $q(\mathbf{z}_s | \mathbf{z}_t, \mathbf{x}) = \mathcal{N}(\mathbf{z}_s; \alpha_s \mathbf{x} + \sqrt{\sigma_s^2 - \sigma_{s|t}^2} \boldsymbol{\epsilon}_t, \sigma_{s|t}^2 \mathbf{I})$. Here, $\sigma_{s|t}^2$ depends on further assumptions. For instance, a Markov forward process leads to $\sigma_{t|s}^2 = \sigma_t^2 - \frac{\alpha_t^2 \sigma_s^2}{\alpha_s^2}$ and $\sigma_{s|t}^2 = \sigma_s^2 - \frac{\alpha_s^2 \sigma_t^2}{\alpha_t^2}$, $\forall s < t$. The reverse process is a parameterized hierarchical model, from which we can sample \mathbf{x} given some condition \mathbf{c} :

$$p_\theta(\mathbf{x} | \mathbf{c}) = \int p_\theta(\mathbf{x} | \mathbf{z}_0) \left[\prod_{t=1}^T p_\theta(\mathbf{z}_{t-1} | \mathbf{z}_t, \mathbf{c}) \right] p_\theta(\mathbf{z}_T | \mathbf{c}) d\mathbf{z}_{0:T}, \quad (2)$$



(a) **Non-diffusion recommender models.** Instead of directly predicting scores s (top-left), DAE (top-right) and VAE (bottom) learn to reconstruct interactions x .



(b) **Diffusion recommender models.** Recent works studied unconditional DMs for CF (top). We incorporate a conditioning mechanism of historical interactions c (bottom).

Figure 2: Graphical models for different recommender models at inference time. Latent variables are colored in blue.

In a simplified setup, $p_\theta(x|z_0)$ is usually chosen to be an identity mapping $p(x|z_0) = \delta(x - z_0)$, and $p_\theta(z_T|c)$ to be a unit Gaussian distribution $p(z_T) = \mathcal{N}(z_T; 0, \mathbf{I})$. The remaining terms are approximated using the transition relations we derived above, *i.e.*, $p_\theta(z_{t-1}|z_t, c) = q(z_{t-1}|z_t, x = \hat{x}_\theta(z_t, c, t))$, $t = 1, \dots, T$. Here, $\hat{x}_\theta(z_t, c, t)$ is a learnable denoising network, or *denoiser*, that is trained to maximize the lower bound of log-likelihood. Typically, the diffusion loss is reduced to the following form:

$$\mathcal{L} = \mathbb{E}_{t \sim \mathcal{U}(1, T), q(z_t|x)} [w_t \|\hat{x}_\theta(z_t, c, t) - x\|^2], \quad (3)$$

where w_t is a weighting factor that balances the gradient magnitude of different timesteps. Intuitively, the reverse process is composed of a series of denoising steps, each of which updates the latent state z_t toward a direction with higher conditional likelihood, and finally arrives at a high-quality sample of x .

CF as an inverse problem. Similar to image inpainting [30] or time series imputation [36], CF can be formulated as an inverse problem and solved using a conditional generative model such as VAE or DM. Denote the set of users as \mathcal{U} and the set of items as \mathcal{I} . For each user in \mathcal{U} , we aim to rank all the items in \mathcal{I} by predicting a score vector $\hat{s} \in \mathbb{R}^{|\mathcal{I}|}$, and then recommend top- K plausible items to fulfill the user’s needs. In the setting of CF with implicit feedback, our supervision is a user-item interaction matrix $X \in \{0, 1\}^{|\mathcal{U}| \times |\mathcal{I}|}$ with each row $x_u \in \{0, 1\}^{|\mathcal{I}|}$ denoting the interaction vector of the user u . The user u has interacted with item i if $x_{u,i} = 1$, whereas no such interaction has been observed if $x_{u,i} = 0$. The difficulty we encounter here is that the true score vector s is not directly available from the binary entries of X . To address this issue, we can follow the paradigm of masked autoencoders (or denoising autoencoders, DAE) as in [46]: (1) for each training interaction vector x , we randomly drop out some of its components to obtain a degraded

version c , and then train an inverse model $p_\theta(x|c)$ to reconstruct x from c ; (2) at inference time, we obtain the predicted scores \hat{s} by reconstructing from u ’s historical interactions x_u . In this way, we implicitly model the expectation $\mathbb{E}[x|c = x_u]$ as the ground-truth scores s . Subsequent works have continued this paradigm, such as Mult-VAE [21], which learned a multinomial $p(x|c)$ by means of variational Bayes. In this paper, we are interested in learning a hierarchical $p(x|c)$ using conditional DM.

Unconditional DM for CF. Before diving into our method, we point out that unconditional DM can be used to solve a certain kind of inverse problems. Specifically, we can model the condition itself as some latent state z_t corrupted by the forward process. Taking CF as an example, Wang et al. [43] assumed an intrinsic Gaussian noise in each x_u , and reconstructed interactions from $p_\theta(x|z_T = x_u)$. Their method instantiates Equation 2 with $p(z_T|c) = \delta(z_T - c)$ and $p_\theta(z_{t-1}|z_t, c) = q(z_{t-1}|z_t, x = \hat{x}_\theta(z_t, t))$, $t = 1, \dots, T$. Notably, they still employed dropout for all the latents z_t during training. As a result, their denoiser $\hat{x}_\theta(z_t, t)$ is forced to invert both the dropout noise and a small-scale Gaussian noise, which can be understood as a robustness-enhanced version of masked autoencoder. In this paper, we decouple the two types of noise and compute each reverse step with user history c as an additional condition. The difference between our modeling method and theirs is illustrated in Figure 2b.

3 PROPOSED METHOD

In this section, we elucidate our modifications of both the forward and reverse processes, leading to a novel DM for CF named GiffCF.

3.1 Graph Signal Forward Process

The high-dimensional and sparse nature of implicit feedback makes it difficult to model the whole distribution of interactions using Gaussian diffusion. Fortunately, recent works have shown that the forward corruption manner of DM is not unique [3, 7, 15, 29]. In the context of recommender systems, our target is to accurately fulfill a user’s needs with predicted items, which is only relevant to $\mathbb{E}[x|c = x_u]$. Therefore, we hypothesize that it is neither efficient nor necessary to rely on Gaussian perturbations to fully explore the distribution of interaction vectors. Rather, we are interested in finding a forward process tailored for implicit feedback data, introducing inductive bias beneficial for CF.

3.1.1 Graph Smoothing with Heat Equation. A user’s interaction vector can be considered a signal on the item-item similarity graph. Inspired by the over-smoothing artifact in GNNs [32], we immediately notice a corruption manner dedicated to graph signals: repeating smoothing operations until it reaches a steady state. Interestingly, similar attempts using blurring filters for forward diffusion have been made in image synthesis literature [15, 29]. The general idea of a smoothing process is to progressively exchange information on a (discretized) Riemannian manifold (*e.g.*, an item-item graph), described by the following continuous-time PDE:

$$\frac{\partial z}{\partial \tau} = \alpha \nabla^2 z, \quad (4)$$

known as the *heat equation*. Intuitively, the Laplacian operator ∇^2 measures the information difference between a point and the average of its neighborhood, and α captures the rate at which

information is exchanged over time τ . For interaction signals, we let $\nabla^2 = \mathbf{A} - \mathbf{I}$ by convention [33], where \mathbf{A} is a normalized adjacency matrix of the item-item graph. It is straightforward to verify the closed form solution of Equation 4 with some initial value $\mathbf{z}(0)$:

$$\begin{aligned} \mathbf{z}(\tau) &= \exp\{-\tau\alpha(\mathbf{I} - \mathbf{A})\}\mathbf{z}(0) \\ &= \mathbf{U} \exp\{-\tau\alpha(1 - \lambda)\} \odot \mathbf{U}^\top \mathbf{z}(0), \quad \tau \geq 0, \end{aligned} \quad (5)$$

where $\mathbf{U} = [\mathbf{u}_1, \dots, \mathbf{u}_{|I|}]$ is the matrix of unit eigenvectors of \mathbf{A} with the corresponding eigenvalues $\lambda = [\lambda_1, \dots, \lambda_{|I|}]$ sorted in descending order, and \odot denotes Hadamard product. The orthonormal matrix \mathbf{U}^\top is often referred to as *graph Fourier transform* (GFT) matrix and \mathbf{U} as its inverse, and the eigenvalues of $-\nabla^2$, i.e. $1 - \lambda$, are called *graph frequencies* [6]. Thus, Equation 5 can be interpreted as exponentially decaying each high-frequency component of the latent signal \mathbf{z} with an anisotropic rate $\alpha(1 - \lambda)$. As $\tau \rightarrow +\infty$, the signal $\mathbf{z}(\tau)$ converges to an over-smoothed steady state $\mathbf{z}(+\infty) = \mathbf{u}_1 \mathbf{u}_1^\top \mathbf{z}(0)$.

A problem of this naive smoothing process is the computational intractability of finding the matrix exponential or fully diagonalizing \mathbf{A} for item-item graphs with thousands and millions of nodes. One solution is to approximate the continuous-time filter in Equation 5 using its first-order Taylor expansion with respect to τ :

$$\exp\{-\tau\alpha(\mathbf{I} - \mathbf{A})\} = (1 - \tau\alpha)\mathbf{I} + \tau\alpha\mathbf{A} + \mathcal{O}(\tau). \quad (6)$$

Here, we simply set $\tau = 1$ for our final state and linearly interpolate the intermediate states to avoid computational overhead, yielding a sequence of forward filters

$$\mathbf{F}_t = (1 - \tau_t\alpha)\mathbf{I} + \tau_t\alpha\mathbf{A}, \quad t = 0, 1, 2, \dots, T, \quad (7)$$

where $0 = \tau_0 < \tau_1 < \dots < \tau_T = 1$ defines a *smoothing schedule*. By multiplying \mathbf{F}_t with the initial interaction signal \mathbf{x} , we obtain a sequence of smoothed preference signals \mathbf{z}_t as the diffusion latent states in the forward process.

Note that by first-order truncation, we only consider 1-hop propagation of message on the item-item graph and do not actually reach the steady state. However, this is sufficient for our purpose, since an over-smoothed latent state may lose personalized information and make marginal improvement to recommendation performance. Unlike the standard Gaussian diffusion that adds noise and destroys useful signals, our forward process itself has the capability of reducing dropout noise and introduces the structure of the interaction space as helpful prior knowledge. This coincides with the idea of graph signal processing techniques for CF [5, 10, 33]. We will later draw inspiration from two strong baselines in this field and design the adjacency matrix \mathbf{A} in Section 3.1.3.

3.1.2 Anisotropic Diffusion in the Graph Spectral Domain. So far, we have introduced a deterministic corruption manner for interaction signals but ignored the probabilistic modeling aspect of DM. To better understand our forward process, we add a Gaussian noise term similar to standard diffusion, yielding the complete formulation of *graph signal forward process*:

$$\begin{aligned} \mathbf{z}_t &= \mathbf{F}_t \mathbf{x} + \sigma_t \boldsymbol{\epsilon}_t, \\ \boldsymbol{\epsilon}_t &\sim \mathcal{N}(\mathbf{0}, \mathbf{I}), \quad t = 0, 1, 2, \dots, T, \end{aligned} \quad (8)$$

where $(\mathbf{F}_t)_{t=1}^T$ is defined in Equation 7 and $(\sigma_t)_{t=1}^T$ controls the noise level. Comparing it with Equation 1, we can see that the mere difference between standard diffusion and ours lies in the

choice of \mathbf{F}_t : the former uses a diagonal matrix $\mathbf{F}_t = \alpha_t \mathbf{I}$ that isotropically decays the interactions, while we adopt a smoothing filter to exchange information on the item-item graph.

To give a further correspondence between the two processes, we diagonalize our filters as

$$\mathbf{F}_t = \mathbf{U}[(1 - \tau_t\alpha)\mathbf{1} + \tau_t\alpha\boldsymbol{\lambda}] \odot \mathbf{U}^\top, \quad t = 0, 1, 2, \dots, T, \quad (9)$$

Let the GFT of \mathbf{x} , \mathbf{z}_t , and $\boldsymbol{\epsilon}_t$ be $\tilde{\mathbf{x}} = \mathbf{U}^\top \mathbf{x}$, $\tilde{\mathbf{z}}_t = \mathbf{U}^\top \mathbf{z}_t$, and $\tilde{\boldsymbol{\epsilon}}_t = \mathbf{U}^\top \boldsymbol{\epsilon}_t$, respectively. By plugging Equation 9 into Equation 8, we get an equivalent formulation of graph signal forward process in the graph spectral domain:

$$\begin{aligned} \tilde{\mathbf{z}}_t &= [(1 - \tau_t\alpha)\mathbf{1} + \tau_t\alpha\boldsymbol{\lambda}] \odot \tilde{\mathbf{x}} + \sigma_t \tilde{\boldsymbol{\epsilon}}_t, \\ \tilde{\boldsymbol{\epsilon}}_t &\sim \mathcal{N}(\mathbf{0}, \mathbf{I}), \quad t = 0, 1, 2, \dots, T. \end{aligned} \quad (10)$$

It turns out to be a special case of Gaussian diffusion with an anisotropic noise schedule; that is, the scalar signal level α_t in Equation 1 now becomes a vector signal level $\boldsymbol{\alpha}_t = (1 - \tau_t\alpha)\mathbf{1} + \tau_t\alpha\boldsymbol{\lambda}$.

3.1.3 Identifying the Item-Item Graph. The interaction matrix \mathbf{X} provides the adjacency between a user node and an item node on the user-item bipartite graph, yet to smooth an interaction vector, it is necessary to measure the similarity between two item nodes. Let us define $\mathbf{D}_U = \text{diagMat}(\mathbf{X}\mathbf{1})$ and $\mathbf{D}_I = \text{diagMat}(\mathbf{X}^\top \mathbf{1})$ as the degree matrices of users and items, respectively. A popular approach to construct an adjacency matrix for the item-item graph is to stack two convolution kernels $\tilde{\mathbf{A}}_{\text{LGN}}$ of LightGCN [12]:

$$\begin{aligned} \tilde{\mathbf{A}}_{\text{LGN}}^2 &= \begin{bmatrix} \mathbf{O} & \mathbf{D}_U^{-\frac{1}{2}} \mathbf{X} \mathbf{D}_I^{-\frac{1}{2}} \\ \mathbf{D}_I^{-\frac{1}{2}} \mathbf{X}^\top \mathbf{D}_U^{-\frac{1}{2}} & \mathbf{O} \end{bmatrix}^2 \\ &= \begin{bmatrix} \mathbf{D}_U^{-\frac{1}{2}} \mathbf{X} \mathbf{D}_I^{-1} \mathbf{X}^\top \mathbf{D}_U^{-\frac{1}{2}} & \mathbf{O} \\ \mathbf{O} & \mathbf{D}_I^{-\frac{1}{2}} \mathbf{X}^\top \mathbf{D}_U^{-1} \mathbf{X} \mathbf{D}_I^{-\frac{1}{2}} \end{bmatrix}, \end{aligned} \quad (11)$$

and then use the lower-right block, which we denote by $\mathbf{A}_{\frac{1}{2}, \frac{1}{2}, \frac{1}{2}}$. More recently, Fu et al. [10] proposed a generalized form of two-step link propagation on the bipartite graph. Here, we reformulate it as an item-item similarity matrix

$$\mathbf{A}_{\beta, \gamma, \delta} = \mathbf{D}_I^{-\delta} \mathbf{X}^\top \mathbf{D}_U^{-\gamma} \mathbf{X} \mathbf{D}_I^{-\beta}, \quad (12)$$

where β, γ, δ are tunable parameters. For example, when $\beta = \gamma = \delta = 0$, the similarity measure degrades into the number of common neighbors between two item nodes [27]. The logic of normalization lies in that nodes with higher degrees often contain less information about their neighbors, and thus should be down-weighted. In our preliminary experiments, we find that using an equal order of normalization on three user/item nodes, i.e. $\beta = \gamma = \delta = \frac{1}{2}$, works consistently better than the LightGCN-style stacking. Therefore, it serves as our default choice.

Nevertheless, this filter only aggregates information from 2-hop neighbors on the original bipartite graph. Breaking this limitation, we strengthen its expressiveness with an ideal low-pass filter similar to GF-CF [33]. Basically, if we denote $\mathbf{U}_{\beta, \gamma, \delta, d}$ as the matrix of eigenvectors corresponding to the top- d eigenvalues of $\mathbf{A}_{\beta, \gamma, \delta}$ (lowest d graph frequencies), the low-pass filter can be decomposed as $\mathbf{U}_{\beta, \gamma, \delta, d} \mathbf{U}_{\beta, \gamma, \delta, d}^\top$. Multiplying it with an interaction vector \mathbf{x} filters out high-frequency components while preserving high-order signals in the low-frequency subspace.

Table 1: A summary of graph filters for interaction signals. \mathbf{x} denotes input and \mathbf{y} denotes filtered output. Scaling factors that do not affect top- K recommendation results are omitted.

Method	Formulation
Linear AE	$\mathbf{y} = \mathbf{W}_{\text{dec}} \mathbf{W}_{\text{enc}} \mathbf{x}, \mathbf{W}_{\text{enc}}, \mathbf{W}_{\text{dec}}^T \in \mathbb{R}^{ I \times d}$
LinkProp [10]	$\mathbf{y} = \mathbf{A}_{\beta, \gamma, \delta} \mathbf{x} = \mathbf{D}_I^{-\delta} \mathbf{X}^T \mathbf{D}_U^{-\gamma} \mathbf{X} \mathbf{D}_I^{-\beta} \mathbf{x}$
GF-CF [33]	$\mathbf{y} = \mathbf{A}_{\text{HE}} \mathbf{x} = \mathbf{A}_{\frac{1}{2}, 1, \frac{1}{2}} \mathbf{x}$ $\mathbf{y} = \mathbf{A}_{\text{IDL}} \mathbf{x} = \mathbf{D}_I^{\frac{1}{2}} \mathbf{U}_{\frac{1}{2}, 1, \frac{1}{2}, d} \mathbf{U}_{\frac{1}{2}, 1, \frac{1}{2}, d}^T \mathbf{D}_I^{-\frac{1}{2}} \mathbf{x}$ $\mathbf{y} = (\mathbf{A}_{\text{HE}} + \omega \mathbf{A}_{\text{IDL}}) \mathbf{x}, \omega \geq 0$
BSPM [†] [5]	$\mathbf{y} = (\mathbf{I} - \omega' \mathbf{A}_{\text{HE}}) (\mathbf{A}_{\text{HE}} + \omega \mathbf{A}_{\text{IDL}}) \mathbf{x}, \omega' \geq 0$
GiffCF (Ours)	$\mathbf{y} = (\mathbf{A}_{\beta, \gamma, \delta} / \ \mathbf{A}_{\beta, \gamma, \delta}\ _2 + \omega \mathbf{U}_{\beta, \gamma, \delta, d} \mathbf{U}_{\beta, \gamma, \delta, d}^T) \mathbf{x}$

[†]Euler method, single blurring/sharpening steps, and early merge.

We summarize representative CF techniques related to graph filters in Table 1. Unifying the designs of LinkProp and GF-CF, we propose the following adjacency matrix in our forward filters:

$$\mathbf{A} = \frac{1}{1 + \omega} \left(\mathbf{A}_{\beta, \gamma, \delta} / \|\mathbf{A}_{\beta, \gamma, \delta}\|_2 + \omega \mathbf{U}_{\beta, \gamma, \delta, d} \mathbf{U}_{\beta, \gamma, \delta, d}^T \right), \quad (13)$$

where d and ω are the cut-off dimension and the strength of ideal low-pass filtering, respectively. Note that the matrix has been scaled to a unit norm.

A note on time complexity. The truncated eigendecomposition can be implemented in a preprocessing stage using efficient algorithms [2, 26]. When applying smoothing filters, the link propagation term requires sparse matrix multiplication and costs $\mathcal{O}(|X|)$ time for each \mathbf{x} , where $|X|$ is the number of observed interactions in the training data; the ideal low-pass term requires low-rank matrix multiplication and costs $\mathcal{O}(|I|d)$ time. Both of them sidestep the need for $\mathcal{O}(|I|^2)$ dense multiplication.

3.2 Graph Signal Reverse Process

As the counterpart of our forward process, we expect a *graph signal reverse process* that iteratively removes the effect of smoothing on the latent preference signals, and finally reconstructs the original interaction vector for recommendation. This is similar to standard diffusion which uses multiple denoising steps to remove Gaussian noise from the latent state. Since we only change the corruption manner of interaction signals, the reverse process of GiffCF is still defined by the hierarchical generative model in Equation 2. And the transition relation between two timesteps t and s can be written as

$$q(\mathbf{z}_s | \mathbf{z}_t, \mathbf{x}) = \mathcal{N}(\mathbf{z}_s; \mathbf{F}_s \mathbf{x} + \sqrt{\sigma_s^2 - \sigma_t^2} \boldsymbol{\epsilon}_t, \sigma_s^2 \mathbf{I}). \quad (14)$$

In this section, we lay the theoretical foundation of this reverse process and detail the implementation of our inference procedure.

3.2.1 Deterministic Sampler. As we have discussed before, noise in the diffusion processes may destroy useful signals and undermine the recommendation performance. Also, the ultimate goal of GiffCF is to give a high-quality estimation of $\mathbb{E}[\mathbf{x} | \mathbf{c}]$, instead of sampling diversified data from the distribution $p_{\theta}(\mathbf{x} | \mathbf{c})$ like in image synthesis. Due to these reasons, we choose to use a deterministic sampler for the reverse process similar to DDIM [35].

Recalling Equation 2 and Equation 14, we assume $\sigma_{t-1|t}^2 = 0$ for all $p_{\theta}(\mathbf{z}_{t-1} | \mathbf{z}_t, \mathbf{c}) = q(\mathbf{z}_{t-1} | \mathbf{z}_t, \mathbf{x} = \hat{\mathbf{x}}_{\theta}(\mathbf{z}_t, \mathbf{c}, t))$, $t = 1, \dots, T$, making each transition from \mathbf{z}_t to \mathbf{z}_{t-1} deterministic:

$$\mathbf{z}_{t-1} = \mathbf{F}_{t-1} \hat{\mathbf{x}}_{\theta} + \frac{\sigma_{t-1}}{\sigma_t} (\mathbf{z}_t - \mathbf{F}_t \hat{\mathbf{x}}_{\theta}), \quad t = 1, \dots, T, \quad (15)$$

where $\hat{\mathbf{x}}_{\theta}(\mathbf{z}_t, \mathbf{c}, t)$ is the denoiser output at the specific timestep t .

For the prior distribution $p(\mathbf{z}_T | \mathbf{c})$, the optimal decision should place all the probability mass on the ground-truth \mathbf{z}_T defined by the forward filter. However, this is not feasible in practice, since we have no access to the true interaction vector \mathbf{x} during inference. To compromise, we approximate \mathbf{z}_T by the smoothed version of historical interactions, *i.e.* $\mathbf{F}_T \mathbf{c}$, because \mathbf{x} and \mathbf{c} should be close enough in the low-frequency subspace, which is exactly the foundational assumption of graph signal processing techniques for CF [33]. The resulting reverse process then becomes a completely deterministic mapping from $\mathbf{F}_T \mathbf{c}$ to \mathbf{x} (see Algorithm 2).

3.2.2 Refining-Sharpener Decomposition. To deepen our understanding of the reverse process, we decompose the update rule of \mathbf{z}_t into a refining term and a sharpening term:

$$\begin{aligned} \mathbf{z}_{t-1} &= [\mathbf{F}_t - (\tau_t - \tau_{t-1})\alpha(\mathbf{A} - \mathbf{I})] \hat{\mathbf{x}}_{\theta} + \frac{\sigma_{t-1}}{\sigma_t} (\mathbf{z}_t - \mathbf{F}_t \hat{\mathbf{x}}_{\theta}) \\ &= \underbrace{\mathbf{z}_t + \left(1 - \frac{\sigma_{t-1}}{\sigma_t}\right) (\mathbf{F}_t \hat{\mathbf{x}}_{\theta} - \mathbf{z}_t)}_{\text{Refining Term}} + \underbrace{(\tau_t - \tau_{t-1})\alpha(\mathbf{I} - \mathbf{A}) \hat{\mathbf{x}}_{\theta}}_{\text{Sharpening Term}}. \end{aligned} \quad (16)$$

Intuitively, the refining term corrects the latent signal \mathbf{z}_t from the previous timestep by a weighted average of $\mathbf{F}_t \hat{\mathbf{x}}_{\theta}$ and \mathbf{z}_t . By tuning the *noise decay* $\frac{\sigma_{t-1}}{\sigma_t}$, we can adjust the amount of refinement at each reverse step. This term can probably ease the negative effect of prior misspecification caused by setting $\mathbf{z}_T = \mathbf{F}_T \mathbf{c}$. Meanwhile, the sharpening term highlights the difference of $\hat{\mathbf{x}}_{\theta}$ from its smoothed version $\mathbf{A} \hat{\mathbf{x}}_{\theta}$, equivalently solving the heat equation in the reverse direction. In our implementation, we use a linear smoothing schedule with $\tau_t = t/T$, $t = 0, 1, \dots, T$, and a constant noise decay $\frac{\sigma_{t-1}}{\sigma_t}$, $t = 1, \dots, T$ as a hyper-parameter to balance the two terms.

3.2.3 Derivation of the Optimization Objective. The denoiser $\hat{\mathbf{x}}_{\theta}$ plays an important role in the reverse process as all the update directions are computed from its output. In order to learn an effective denoiser for high-quality reconstruction, we try to maximize the conditional log-likelihood of the generated data:

$$\begin{aligned} \log p_{\theta}(\mathbf{x} | \mathbf{c}) &= \log \mathbb{E}_{q(\mathbf{z}_{0:T} | \mathbf{x})} \left[\frac{p_{\theta}(\mathbf{z}_{0:T}, \mathbf{x} | \mathbf{c})}{q(\mathbf{z}_{0:T} | \mathbf{x})} \right] \\ &\geq \mathbb{E}_{q(\mathbf{z}_{0:T} | \mathbf{x})} \left[\log \frac{p_{\theta}(\mathbf{z}_{0:T}, \mathbf{x} | \mathbf{c})}{q(\mathbf{z}_{0:T} | \mathbf{x})} \right] \\ &= - \underbrace{D_{\text{KL}}(q(\mathbf{z}_T | \mathbf{x}) \parallel p(\mathbf{z}_T | \mathbf{c}))}_{\text{Prior Loss}} - \underbrace{\mathbb{E}_{q(\mathbf{z}_0 | \mathbf{x})} [-\log p(\mathbf{x} | \mathbf{z}_0)]}_{\text{Reconstruction Loss}} \\ &\quad - \underbrace{\sum_{t=1}^T \mathbb{E}_{q(\mathbf{z}_t | \mathbf{x})} [D_{\text{KL}}(q(\mathbf{z}_{t-1} | \mathbf{z}_t, \mathbf{x}) \parallel p_{\theta}(\mathbf{z}_{t-1} | \mathbf{z}_t, \mathbf{c}))]}_{\text{Diffusion Loss}}. \end{aligned} \quad (17)$$

Algorithm 1: GiffCF training.**Input:** Interaction matrix X .1 **repeat**2 Sample u from \mathcal{U} and let $\mathbf{x} \leftarrow \mathbf{x}_u$.3 Randomly drop out \mathbf{x} to obtain \mathbf{c} .4 Sample $t \sim \mathcal{U}(1, T)$ and $\mathbf{z}_t \sim \mathcal{N}(F_t \mathbf{x}, \sigma_t^2 \mathbf{I})$.5 Take a gradient step on $\nabla_{\theta} \|\hat{\mathbf{x}}_{\theta}(\mathbf{z}_t, \mathbf{c}, t) - \mathbf{x}\|^2$.6 **until** converged;**Output:** Denoiser parameters θ .

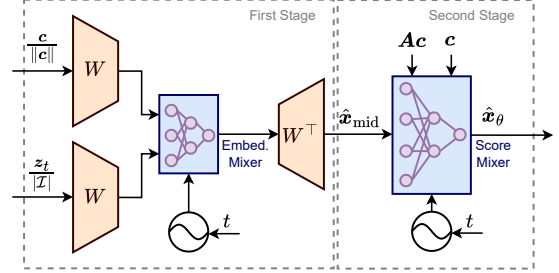
The right-hand side of the above inequality is known as the *variational lower bound* (VLB) [17] of log-likelihood. Since we set $p(\mathbf{z}_T | \mathbf{c}) = \delta(\mathbf{z}_T - F_T \mathbf{c})$ and $p(\mathbf{x} | \mathbf{z}_0) = \delta(\mathbf{x} - \mathbf{z}_0)$ in practice, the prior loss and reconstruction loss are both constant and can be ignored during optimization. We will now derive an estimator for the diffusion loss. Since $q(\mathbf{z}_{t-1} | \mathbf{z}_t, \mathbf{x})$ and $p_{\theta}(\mathbf{z}_{t-1} | \mathbf{z}_t, \mathbf{c})$ are both Gaussian, the KL divergence can be computed in a closed form:

$$\begin{aligned} & D_{\text{KL}}(q(\mathbf{z}_s | \mathbf{z}_t, \mathbf{x}) \parallel p_{\theta}(\mathbf{z}_s | \mathbf{z}_t, \mathbf{c})) \\ &= \frac{1}{2\sigma_{s|t}^2} \|\mathbf{F}_s(\hat{\mathbf{x}}_{\theta} - \mathbf{x}) + \sqrt{\sigma_s^2 - \sigma_{s|t}^2}(\hat{\epsilon}_{\theta} - \epsilon_t)\|^2. \\ &= \frac{1}{2\sigma_{s|t}^2} \left\| \left(\mathbf{F}_s - \sqrt{\sigma_s^2 - \sigma_{s|t}^2} / \sigma_t \cdot \mathbf{F}_t \right) (\hat{\mathbf{x}}_{\theta} - \mathbf{x}) \right\|^2. \\ &\leq \frac{1}{2\sigma_{s|t}^2} \left\| \mathbf{F}_s - \sqrt{\sigma_s^2 - \sigma_{s|t}^2} / \sigma_t \cdot \mathbf{F}_t \right\|^2 \|\hat{\mathbf{x}}_{\theta} - \mathbf{x}\|^2 = C_{s|t} \|\hat{\mathbf{x}}_{\theta} - \mathbf{x}\|^2, \end{aligned} \quad (18)$$

where $\hat{\epsilon}_{\theta} = (\mathbf{z}_t - F_t \hat{\mathbf{x}}_{\theta}) / \sigma_t$. The inequality is due to the compatibility between the matrix and vector norms. Therefore, the total loss reduces to a summation of T weighted square errors. Following the standard practice of DM, we sample the timestep t uniformly at random and minimize a reweighted version of the diffusion loss, which is identical to the loss of standard DM (see Equation 3).

While image DMs typically learn a U-Net [31] denoiser for predicting ϵ_t and essentially set w_t to the signal-to-noise ratio $\frac{\alpha_t^2}{\sigma_t^2}$ [17], in this paper, we choose to directly predict \mathbf{x} with $w_t = 1$ for all $t = 1, \dots, T$, as we find it more stable when used in conjunction with our denoiser architecture.

3.2.4 Denoiser Architecture. We adopt a two-stage design of the denoiser $\hat{\mathbf{x}}_{\theta}$. (1) In the first stage, the network encodes both the latent preference signal \mathbf{z}_t and the historical interaction signal \mathbf{c} by multiplying them with a shared item embedding matrix $\mathbf{W} \in \mathbb{R}^{|\mathcal{I}| \times d}$ after proper normalization. The embeddings are then concatenated and fed into an item-wise MLP to mix information from the two sources. To account for timestep information, we also concatenate a timestep embedding to the input of the MLP. After that, the mixed embedding is decoded back into the interaction space by multiplying with the transposed item embedding matrix \mathbf{W}^T . This decoding operation can be seen as a dot product between the mixed user embedding and each item embedding in \mathbf{W} , which is a common practice in matrix-factorization models [19]. (2) In the second stage, we concatenate the intermediate score vector \mathbf{x}_{mid} from the first stage with the historical interaction vector \mathbf{c} and its smoothed version \mathbf{Ac} , and feed them into another item-wise MLP to predict the

Algorithm 2: GiffCF inference.**Input:** θ and historical interactions \mathbf{x}_u of a user u .1 Let $\mathbf{c} \leftarrow \mathbf{x}_u$ and $\mathbf{z}_T \leftarrow F_T \mathbf{c}$.2 **for** $t = T, \dots, 1$ **do**3 Predict $\hat{\mathbf{x}}_{\theta} \leftarrow \hat{\mathbf{x}}_{\theta}(\mathbf{z}_t, \mathbf{c}, t)$.4 Update $\mathbf{z}_{t-1} \leftarrow F_{t-1} \hat{\mathbf{x}}_{\theta} + \sigma_{t-1} / \sigma_t (\mathbf{z}_t - F_t \hat{\mathbf{x}}_{\theta})$.5 **end**6 Let $\mathbf{x} \leftarrow \mathbf{z}_0$.**Output:** Predicted preference scores \mathbf{x} .**Figure 3:** The architecture of the denoiser $\hat{\mathbf{x}}_{\theta}$ in GiffCF.

final interaction vector $\hat{\mathbf{x}}_0$. Again, we concatenate a timestep embedding to the input of the MLP. The trainable parameters include the item embedding matrix \mathbf{W} and four MLPs: embedding mixer, score mixer, and two timestep encoders on the sinusoidal basis. The sizes of two mixers are shown in Figure 3. All the MLPs have one hidden layer with Swish activation. The overall architecture is illustrated in Figure 3.

4 EXPERIMENTS

In this section, we conduct experiments on three real-world datasets to verify the effectiveness of GiffCF. We aim to answer the following research questions:

- **RQ1** How does GiffCF perform compared to state-of-the-art baselines, including diffusion recommender models and graph signal processing techniques?
- **RQ2** How does the number of diffusion steps T , the smoothing schedule (controlled by α), and the noise schedule (controlled by σ_T) affect the performance of GiffCF?
- **RQ3** How does the reverse process iteratively improve the recommendation results? Does our design of the denoiser architecture contribute to its performance?

4.1 Experimental Setup

4.1.1 Datasets. For a fair comparison, we use the same preprocessed and split versions of three public datasets suggested by [43]:

- **MovieLens-1M** contains 571,531 interactions among 5,949 users and 2,810 items with a sparsity of 96.6%.
- **Yelp** contains 1,402,736 interactions among 54,574 users and 34,395 items with a sparsity of 99.93%.
- **Amazon-Book** contains 3,146,256 interactions among 108,822 users and 94,949 items with a sparsity of 99.97%.

Table 2: Performance comparison on all three datasets. The best results are highlighted in bold and the second-best results are underlined. %Improv. represents the relative improvements of GiffCF over the best baseline results. * implies the improvements over the best baseline are statistically significant (p -value < 0.05) under one-sample t-tests.

Dataset	Metric	MF	LightGCN	Mult-VAE	DiffRec	L-DiffRec	LinkProp	GF-CF	BSPM	GiffCF	%Improv.
MovieLens-1M	Recall@10	0.0885	0.1112	0.1170	<u>0.1178</u>	0.1174	0.1039	0.1088	0.1107	0.1251*	6.17%
	Recall@20	0.1389	0.1798	0.1833	0.1827	<u>0.1847</u>	0.1509	0.1718	0.1740	0.1947*	5.44%
	NDCG@10	0.0680	0.0838	0.0898	<u>0.0901</u>	0.0868	0.0852	0.0829	0.0838	0.0962*	6.76%
	NDCG@20	0.0871	0.1089	<u>0.1149</u>	0.1148	0.1122	0.1031	0.1067	0.1079	0.1221*	6.28%
	MRR@10	0.1202	0.1363	0.1493	<u>0.1507</u>	0.1394	0.1469	0.1383	0.1388	0.1577*	4.63%
	MRR@20	0.1325	0.1495	0.1616	<u>0.1630</u>	0.1520	0.1574	0.1505	0.1513	0.1704*	4.53%
Yelp	Recall@10	0.0509	0.0629	0.0595	0.0586	0.0589	0.0604	0.0630	<u>0.0630</u>	0.0648*	2.92%
	Recall@20	0.0852	<u>0.1041</u>	0.0979	0.0961	0.0971	0.0980	0.1029	0.1033	0.1063*	2.12%
	NDCG@10	0.0301	0.0379	0.0360	0.0363	0.0353	0.0370	0.0381	<u>0.0382</u>	0.0397*	3.88%
	NDCG@20	0.0406	0.0504	0.0477	0.0487	0.0469	0.0485	0.0502	<u>0.0505</u>	0.0523*	3.59%
	MRR@10	0.0354	0.0446	0.0425	0.0445	0.0411	0.0445	0.0451	<u>0.0452</u>	0.0476*	5.34%
	MRR@20	0.0398	0.0497	0.0474	0.0493	0.0460	0.0493	0.0501	<u>0.0503</u>	0.0527*	4.84%
Amazon-Book	Recall@10	0.0686	0.0699	0.0688	0.0700	0.0697	<u>0.1087</u>	0.1049	0.1055	0.1121*	3.08%
	Recall@20	0.1037	0.1083	0.1005	0.1011	0.1029	<u>0.1488</u>	0.1435	0.1435	0.1528*	2.69%
	NDCG@10	0.0414	0.0421	0.0424	0.0451	0.0440	<u>0.0709</u>	0.0688	0.0696	0.0733*	3.32%
	NDCG@20	0.0518	0.0536	0.0520	0.0547	0.0540	<u>0.0832</u>	0.0807	0.0814	0.0858*	3.16%
	MRR@10	0.0430	0.0443	0.0455	0.0502	0.0468	0.0762	0.0750	<u>0.0763</u>	0.0795*	4.15%
	MRR@20	0.0471	0.0487	0.0482	0.0540	0.0506	0.0807	0.0795	<u>0.0808</u>	0.0842*	4.16%

Each dataset is split into training, validation, and testing sets with a ratio of 7:1:2. For each trainable method, we use the validation set to select the best epoch and the testing set to tune the hyper-parameters and get the final results. To evaluate the top- K recommendation performance, we report the average Recall@ K (normalized as in [21]), NDCG@ K [11, 13], and MRR@ K [4, 38] among all the users, where we set $K \in \{10, 20\}$.

4.1.2 Baselines. The following baseline methods are considered:

- **MF** [19] & **LightGCN** [12], two representative recommender models that optimize the BPR loss [28]. The latter linearly aggregates embeddings on the user-item bipartite graph.
- **Mult-VAE** [21], which generates interaction vectors from a multinomial distribution using variational inference.
- **DiffRec** & **L-DiffRec** [43], unconditional diffusion recommender models with standard Gaussian diffusion. The latter generates the embedding of an interaction vector encoded by grouped VAEs.
- **LinkProp** [10] & **GF-CF** [33] & **BSPM** [5], graph signal processing techniques for CF (see Table 1), which proved to outperform embedding-based models on large sparse datasets. The last one also simulates the heat equation with a sharpening process.

4.1.3 Hyper-parameters. For DiffRec and L-DiffRec, we reuse the checkpoints released by the authors, which are tuned in a vast search space. For the other baselines, we set all the user/item embedding sizes, hidden layer sizes, cut-off dimensions of ideal low-pass filters to 200. The dropout rates for Mult-VAE and all diffusion models are set to 0.5. Hyper-parameters not mentioned above are tuned or set to the default values suggested in the original papers. For our own model, by default, we set $\beta = \gamma = \delta = \frac{1}{2}$ for item-item similarities, $T = 3$ as the number of diffusion steps, $\alpha = 1.5$ as the smoothing strength, $\sigma_T = 0$ as the noise scale, and tune the ideal low-pass filters weight ω in $\{0.0, 0.1, 0.2, 0.3\}$, the noise decay $\frac{\sigma_{T-1}}{\sigma_T}$

in $\{0.1, 0.5, 1.0\}$. We optimize all the models using Adam [18] with a constant learning rate in $\{10^{-5}, 10^{-4}, 10^{-3}\}$.

We implement GiffCF in Python 3.11 and Tensorflow 2.14. All the models are trained on a single RTX 3080 Ti GPU. For more details, please refer to our released code.

4.2 Comparison with the State-of-the-Art

The overall performance of GiffCF and the baselines on all three datasets is in Table 2. The following observations can be made:

- All baseline models based on user/item embeddings (MF, LightGCN, Mult-VAE, DiffRec, L-DiffRec) show competitive performance on small datasets. However, on the larger and sparser Amazon-Book dataset, there is a significant performance drop compared to graph signal processing techniques (LinkProp, GF-CF, BSPM). This is because decomposing the high-dimensional interaction matrix into low-rank embedding matrices loses a lot of detailed information. As a result, these models struggle to capture the complex structure of the interaction space.
- When the number of parameters is comparable and training is sufficient, previous DMs for CF (DiffRec, L-DiffRec) do not exhibit a significant advantage over simpler baselines. This suggests that there is plenty of room for improvement in the design of DM and necessitates the introduction of more advanced techniques.
- GiffCF outperforms all the baselines on all the metrics on all the datasets. The superiority of GiffCF can be attributed to (1) the helpful prior knowledge of the interaction space structure introduced by advanced graph signal smoothing filters; (2) the hierarchical reconstruction of the interaction vector via refining and sharpening in the reverse process; (3) the two-stage denoiser effectively mixing different sources of information. We will analyze the effectiveness of each component in later sections.

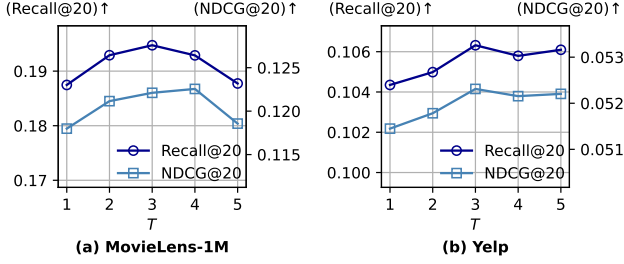


Figure 4: Effect of the number of diffusion steps T .

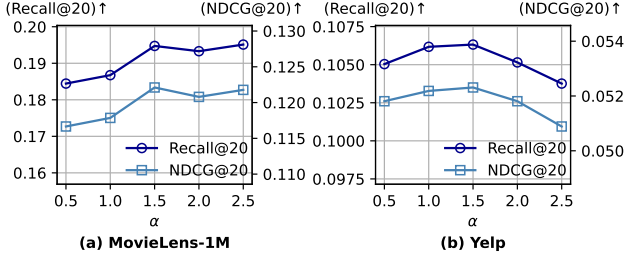


Figure 5: Effect of the smoothing strength α .

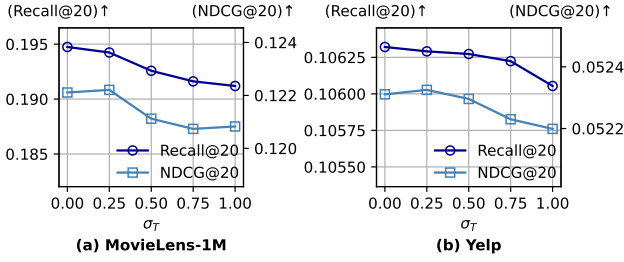


Figure 6: Effect of the noise scale σ_T .

4.3 Sensitivity on the Diffusion Schedule

To demonstrate the effectiveness of graph signal diffusion and to provide guidance on scheduling-related hyper-parameter selection, we conduct sensitivity analysis on the number of diffusion steps T , the smoothing strength α , and the noise scale σ_T .

4.3.1 Effect of T . We varied the number of diffusion steps T from 1 to 5 and trained GiffCF from scratch. From the results in Figure 4, we can see that (1) as T increases, the model performance first rises significantly, highlighting the advantage of a hierarchical generative model over those with a single latent variable. (2) beyond 3 steps, some performance metrics exhibit oscillations or declines, implying that an excessive number of sampling steps will not necessarily lead to higher accuracy. This bottleneck could stem from the limited expressiveness of the denoiser or potential inaccuracy in the prior estimation. Considering the computational burden associated with increasing steps, we suggest a uniform choice of $T = 3$ to achieve near-optimal performance with acceptable execution time.

4.3.2 Effect of α . The smoothing strength α describes the extent of information exchange in graph signal forward process, analogous to thermal diffusivity in a physical heat equation. To inspect its effect, we compare the results with α changing from 0.5 to 2.5 at an interval of 0.5. Quite similar to the effect of T , we observe that the performance first increases and then oscillates or declines as α exceeds 1.5, suggesting that a moderate smoothing strength is preferred. We interpret this phenomenon as follows: when α is below a certain threshold, z_T may be under-smoothed and entangled with the original signal; when α is too large, z_T may be over-smoothed and amplifying the difference between Ax and x in an erroneous way. Both circumstances can impede the denoiser from discerning the hierarchical information within latent variables, ultimately leading to suboptimal performance. Based on experiments, $\alpha = 1.5$ is a good choice overall.

4.3.3 Effect of σ_T . As discussed earlier, adding Gaussian noise in the diffusion process is not necessary for CF and poses a risk of information loss. To verify the effect of noise scale σ_T on graph signal diffusion, we compare the results with σ_T changing from 0.0 to 1.0 at an interval of 0.2. The results in Figure 6 clearly illustrate that with an increase in the noise scale, the model performance shows a declining trend. Hence, we suggest abandoning the noise term in the forward process. In this way, we allow the model to attend to and learn from clean and smoothed preference signals, making GiffCF a noise-free DM. It should be noted that even though we set the noise scale to zero, we still define the noise decay $\frac{\sigma_{t-1}}{\sigma_t}$ to control the refining term in graph signal reverse process. We will analyze the role of $\frac{\sigma_{t-1}}{\sigma_t}$ in the next section.

4.4 Analysis of the Reverse Process

4.4.1 Role of the Refining Term. In Section 3.2.2, there is a so-called refining term that updates the previous latent signal z_t toward a refined prediction $F_t \hat{x}_\theta$. To understand it from an empirical perspective, we change the ratio $\frac{\sigma_{t-1}}{\sigma_t}$ during inference and see how the model performs. The results are in Figure 7. On Yelp, we find that the smaller $\frac{\sigma_{t-1}}{\sigma_t}$, the better the performance. On Amazon-Book, the opposite trend is observed. In short, this is because embedding-based denoiser performs better on smaller datasets. In this case, setting $\frac{\sigma_{t-1}}{\sigma_t}$ to a small value can emphasize the refinement and mitigate the misspecification of the prior z_T . On larger and sparser datasets, preserving $F_T c$ as a prior estimate proves to be more beneficial, and hence setting $\frac{\sigma_{t-1}}{\sigma_t}$ near 1.0 is preferred.

4.4.2 Quality of the Sampling Trajectory. To show that the reverse process is indeed improving the preference scores through iterative refining and sharpening, we evaluate the quality of the sampling trajectory $z_t, t = T, \dots, 0$ in terms of the recommendation performance. The results in Figure 8 show that z_t progressively produces better results after each sampling step, which validates the effectiveness of graph signal reverse process.

4.4.3 Ablation on the Denoiser Architecture. Another important finding is that the denoiser architecture plays a crucial role in the performance of GiffCF. To verify this, we conduct ablation studies by either removing z_t in the first stage (w/o latent), removing c in the first stage (w/o pre-cond), or removing Ac and c in the second stage (w/o post-cond). The results in Table 3 show that both

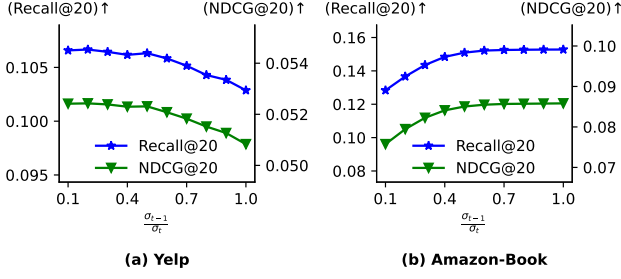


Figure 7: Effect of the noise decay $\frac{\sigma_{t-1}}{\sigma_t}$ (which controls the refining term in Equation 16) during reverse sampling.

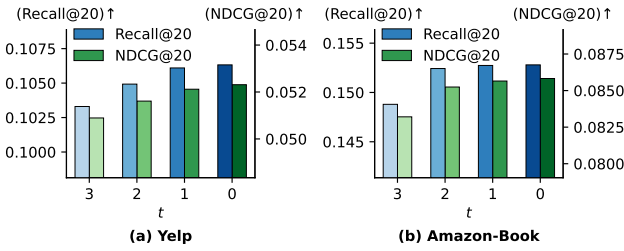


Figure 8: Recommendation performance using latent signals z_t at each reverse sampling step t .

Table 3: Ablation studies on the denoiser architecture. The best results are highlighted in bold.

Dataset	Arch. of \hat{x}_θ	Recall@20	NDCG@20	MRR@20
MovieLens-1M	-	0.1947	0.1221	0.1704
	w/o latent	0.1667	0.1105	0.1639
	w/o pre-cond	0.1829	0.1159	0.1648
	w/o post-cond	0.1888	0.1204	0.1698
Yelp	-	0.1063	0.0523	0.0527
	w/o latent	0.1055	0.0520	0.0522
	w/o pre-cond	0.1041	0.0509	0.0512
	w/o post-cond	0.0851	0.0418	0.0431
Amazon-Book	-	0.1528	0.0858	0.0842
	w/o latent	0.1506	0.0846	0.0827
	w/o pre-cond	0.1518	0.0850	0.0829
	w/o post-cond	0.1057	0.0570	0.0556

components are indispensable for achieving the best performance, consistent with our intuition. On the one hand, the information from both z_t and c can encourage learning a better embedding matrix W that utilizes the prior knowledge from the forward process. On the other hand, feeding A_c and c into a final item-wise mixer can help the denoiser remove the artifacts caused by low-rank compression. This is especially important for high-dimensional datasets, where a solely embedding-based model is prone to underfitting. To sum up, the two-stage denoiser architecture effectively mixes different sources of information from z_t and c .

5 RELATED WORKS

The related works can be classified into two categories: DM for recommendation and DM with general corruption.

DM for recommendation. As a powerful family of generative models, DM has recently garnered attention in the field of recommender systems. Most of these models rely on Gaussian noise to explore either the interaction or the user/item embedding space, encompassing the subfields of CF [37, 43], sequential recommendation [8, 20, 23, 45, 47], *etc.* An exception to this trend is the use of discrete diffusion for multi-stage recommendation [22]. For CF, non-Gaussian diffusion in the interaction space is still under-explored. Notably, Choi et al. [5] designed a graph signal processing technique inspired by DM, which also involves a sharpening process to improve recommendation performance. Our work stands out as the first to incorporate graph signal processing into the theoretical framework of DM for CF, thereby achieving the best of both worlds.

DM with general corruption. Researchers have been exploring general forms of corruption in DM. For example, Bansal et al. [3] explored cold DM without noise; Daras et al. [7] explored DM with general linear operators; Rissanen et al. [29] and Hoogetboom and Salimans [15] explored DM with image blurring filters; Austin et al. [1] explored discrete DM with general transition probabilities; *etc.* We are the first to propose DM with graph smoothing filters for implicit feedback data, contributing to a general corruption form for graph-structured continuous state spaces.

6 CONCLUSION AND FUTURE WORK

In this work, we present GiffCF, a novel DM for CF that smooths and sharpens graph signals by simulating the heat equation. The proposed hierarchical generative model effectively leverages the adjacency of the item-item similarity graph and enables high-quality reconstruction of user-item interactions. Extensive experiments not only demonstrate the superiority of our method compared to the state-of-the-art, but also provide empirical insights into the design of several key components. We believe that GiffCF can serve as a strong baseline for future recommender systems research.

To extend our work, one can consider: (1) designing more powerful denoisers or training strategies to accelerate convergence and enhance performance; (2) integrating other conditional information, such as user demographics, to better control the reverse process; (3) adapting our model to other types of recommendation tasks, probably by exploring similar corruption forms in the embedding space. Hopefully, our work could inspire more researchers to think beyond the boundaries of conventional image DMs and design task-specific DMs with general corruption. By that means, we can truly unleash the potential of DM in information retrieval.

ACKNOWLEDGMENTS

This work was partially supported by National Natural Science Foundation of China (Grant No.92370204), Guangzhou-HKUST(GZ) Joint Funding Program (Grant No.2023A03J0008), Education Bureau of Guangzhou Municipality, and Guangdong Science and Technology Department. It was also partially supported by China Postdoctoral Science Foundation (Grant No.2023M730785) and China Postdoctoral Science Foundation (Grant No.2023M741849).

REFERENCES

- [1] Jacob Austin, Daniel D. Johnson, Jonathan Ho, Daniel Tarlow, and Rianne van den Berg. 2021. Structured Denoising Diffusion Models in Discrete State-Spaces. In *Advances in Neural Information Processing Systems*, Vol. 34. Curran Associates, Inc., 17981–17993.
- [2] James Baglama and Lothar Reichel. 2005. Augmented Implicitly Restarted Lanczos Bidiagonalization Methods. *SIAM Journal on Scientific Computing* 27, 1 (Jan. 2005), 19–42. <https://doi.org/10.1137/04060593X>
- [3] Arpit Bansal, Eitan Borgnia, Hong-Min Chu, Jie Li, Hamid Kazemi, Furong Huang, Micah Goldblum, Jonas Geiping, and Tom Goldstein. 2023. Cold Diffusion: Inverting Arbitrary Image Transforms Without Noise. *Advances in Neural Information Processing Systems* 36 (Dec. 2023), 41259–41282.
- [4] Dong-Kyu Chae, Jin-Soo Kang, Sang-Wook Kim, and Jung-Tae Lee. 2018. CFGAN: A Generic Collaborative Filtering Framework Based on Generative Adversarial Networks. In *Proceedings of the 27th ACM International Conference on Information and Knowledge Management (CIKM '18)*. Association for Computing Machinery, New York, NY, USA, 137–146. <https://doi.org/10.1145/3269206.3271743>
- [5] Jeongwhan Choi, Seoyoung Hong, Noseong Park, and Sung-Bae Cho. 2023. Blurring-Sharpener Process Models for Collaborative Filtering. In *Proceedings of the 46th International ACM SIGIR Conference on Research and Development in Information Retrieval (SIGIR '23)*. Association for Computing Machinery, New York, NY, USA, 1096–1106. <https://doi.org/10.1145/3539618.3591645>
- [6] Fan R. K. Chung. [n. d.]. *Spectral Graph Theory*. American Mathematical Soc.
- [7] Giannis Daras, Mauricio Delbracio, Hossein Talebi, Alexandros G. Dimakis, and Peyman Milanfar. 2022. Soft Diffusion: Score Matching for General Corruptions. <https://doi.org/10.48550/arXiv.2209.05442> arXiv:2209.05442 [cs]
- [8] Hanwen Du, Huanhuan Yuan, Zhen Huang, Pengpeng Zhao, and Xiaofang Zhou. 2023. Sequential Recommendation with Diffusion Models. <https://doi.org/10.48550/arXiv.2304.04541> arXiv:2304.04541 [cs]
- [9] Wenqi Fan, Xiaorui Liu, Wei Jin, Xiangyu Zhao, Jiliang Tang, and Qing Li. 2022. Graph Trend Filtering Networks for Recommendation. In *Proceedings of the 45th International ACM SIGIR Conference on Research and Development in Information Retrieval (SIGIR '22)*. Association for Computing Machinery, New York, NY, USA, 112–121. <https://doi.org/10.1145/3477495.3531985>
- [10] Hao-Ming Fu, Patrick Poirson, Kwot Sin Lee, and Chen Wang. 2022. Revisiting Neighborhood-based Link Prediction for Collaborative Filtering. In *Companion Proceedings of the Web Conference 2022 (WWW '22)*. Association for Computing Machinery, New York, NY, USA, 1009–1018. <https://doi.org/10.1145/3487553.3524712>
- [11] Xiangnan He, Tao Chen, Min-Yen Kan, and Xiao Chen. 2015. TriRank: Review-aware Explainable Recommendation by Modeling Aspects. In *Proceedings of the 24th ACM International Conference on Information and Knowledge Management (CIKM '15)*. Association for Computing Machinery, New York, NY, USA, 1661–1670. <https://doi.org/10.1145/2806416.2806504>
- [12] Xiangnan He, Kuan Deng, Xiang Wang, Yan Li, YongDong Zhang, and Meng Wang. 2020. LightGCN: Simplifying and Powering Graph Convolution Network for Recommendation. In *Proceedings of the 43rd International ACM SIGIR Conference on Research and Development in Information Retrieval (SIGIR '20)*. Association for Computing Machinery, New York, NY, USA, 639–648. <https://doi.org/10.1145/3397271.3401063>
- [13] Xiangnan He, Lizi Liao, Hanwang Zhang, Liqiang Nie, Xia Hu, and Tat-Seng Chua. 2017. Neural Collaborative Filtering. In *Proceedings of the 26th International Conference on World Wide Web (WWW '17)*. International World Wide Web Conferences Steering Committee, Republic and Canton of Geneva, CHE, 173–182. <https://doi.org/10.1145/3038912.3052569>
- [14] Jonathan Ho, Ajay Jain, and Pieter Abbeel. 2020. Denoising Diffusion Probabilistic Models. In *Advances in Neural Information Processing Systems*, Vol. 33. Curran Associates, Inc., 6840–6851.
- [15] Emiel Hoogeboom and Tim Salimans. 2022. Blurring Diffusion Models. In *The Eleventh International Conference on Learning Representations*.
- [16] Yifan Hu, Yehuda Koren, and Chris Volinsky. 2008. Collaborative Filtering for Implicit Feedback Datasets. In *2008 Eighth IEEE International Conference on Data Mining*, 263–272. <https://doi.org/10.1109/ICDM.2008.22>
- [17] Diederik Kingma, Tim Salimans, Ben Poole, and Jonathan Ho. 2021. Variational Diffusion Models. In *Advances in Neural Information Processing Systems*, Vol. 34. Curran Associates, Inc., 21696–21707.
- [18] Diederik P. Kingma and Jimmy Ba. 2017. Adam: A Method for Stochastic Optimization. <https://doi.org/10.48550/arXiv.1412.6980> arXiv:1412.6980 [cs]
- [19] Yehuda Koren, Robert Bell, and Chris Volinsky. 2009. Matrix Factorization Techniques for Recommender Systems. *Computer* 42, 8 (Aug. 2009), 30–37. <https://doi.org/10.1109/MC.2009.263>
- [20] Zihao Li, Aixin Sun, and Chenliang Li. 2023. DiffuRec: A Diffusion Model for Sequential Recommendation. *ACM Transactions on Information Systems* 42, 3 (Dec. 2023), 66:1–66:28. <https://doi.org/10.1145/3631116>
- [21] Dawen Liang, Rahul G. Krishnan, Matthew D. Hoffman, and Tony Jebara. 2018. Variational Autoencoders for Collaborative Filtering. In *Proceedings of the 2018 World Wide Web Conference (WWW '18)*. International World Wide Web Conferences Steering Committee, Republic and Canton of Geneva, CHE, 689–698. <https://doi.org/10.1145/3178876.3186150>
- [22] Xiao Lin, Xiaokai Chen, Chenyang Wang, Hantao Shu, Linfeng Song, Biao Li, and Peng Jiang. 2023. Discrete Conditional Diffusion for Reranking in Recommendation. <https://doi.org/10.48550/arXiv.2308.06982> arXiv:2308.06982 [cs]
- [23] Qidong Liu, Fan Yan, Xiangyu Zhao, Zhaocheng Du, Hui Feng Guo, Ruiming Tang, and Feng Tian. 2023. Diffusion Augmentation for Sequential Recommendation. In *Proceedings of the 32nd ACM International Conference on Information and Knowledge Management (CIKM '23)*. Association for Computing Machinery, New York, NY, USA, 1576–1586. <https://doi.org/10.1145/3583780.3615134>
- [24] Yen-Ju Lu, Zhong-Qiu Wang, Shinji Watanabe, Alexander Richard, Cheng Yu, and Yu Tsao. 2022. Conditional Diffusion Probabilistic Model for Speech Enhancement. In *ICASSP 2022 - 2022 IEEE International Conference on Acoustics, Speech and Signal Processing (ICASSP)*. 7402–7406. <https://doi.org/10.1109/ICASSP43922.2022.9746901>
- [25] Jianxin Ma, Chang Zhou, Peng Cui, Hongxia Yang, and Wenwu Zhu. 2019. Learning Disentangled Representations for Recommendation. In *Advances in Neural Information Processing Systems*, Vol. 32. Curran Associates, Inc.
- [26] Cameron Musco and Christopher Musco. 2015. Randomized Block Krylov Methods for Stronger and Faster Approximate Singular Value Decomposition. In *Advances in Neural Information Processing Systems*, Vol. 28. Curran Associates, Inc.
- [27] M. E. J. Newman. 2001. Clustering and Preferential Attachment in Growing Networks. *Physical Review E* 64, 2 (July 2001), 025102. <https://doi.org/10.1103/PhysRevE.64.025102>
- [28] Steffen Rendle, Christoph Freudenthaler, Zeno Gantner, and Lars Schmidt-Thieme. 2009. BPR: Bayesian Personalized Ranking from Implicit Feedback. In *Proceedings of the Twenty-Fifth Conference on Uncertainty in Artificial Intelligence (UAI '09)*. AUAI Press, Arlington, Virginia, USA, 452–461.
- [29] Severi Rissanen, Markus Heinonen, and Arno Solin. 2022. Generative Modelling with Inverse Heat Dissipation. In *The Eleventh International Conference on Learning Representations*.
- [30] Robin Rombach, Andreas Blattmann, Dominik Lorenz, Patrick Esser, and Björn Ommer. 2022. High-Resolution Image Synthesis With Latent Diffusion Models. In *Proceedings of the IEEE/CVF Conference on Computer Vision and Pattern Recognition*. 10684–10695.
- [31] Olaf Ronneberger, Philipp Fischer, and Thomas Brox. 2015. U-Net: Convolutional Networks for Biomedical Image Segmentation. In *Medical Image Computing and Computer-Assisted Intervention – MICCAI 2015*, Nassir Navab, Joachim Hornegger, William M. Wells, and Alejandro F. Frangi (Eds.). Springer International Publishing, Cham, 234–241. https://doi.org/10.1007/978-3-319-24574-4_28
- [32] T. Konstantin Rusch, Michael M. Bronstein, and Siddhartha Mishra. 2023. A Survey on Oversmoothing in Graph Neural Networks. <https://doi.org/10.48550/arXiv.2303.10993> arXiv:2303.10993 [cs]
- [33] Yifei Shen, Yongji Wu, Yao Zhang, Caihua Shan, Jun Zhang, B. Khaled Letaief, and Dongsheng Li. 2021. How Powerful Is Graph Convolution for Recommendation?. In *Proceedings of the 30th ACM International Conference on Information & Knowledge Management (CIKM '21)*. Association for Computing Machinery, New York, NY, USA, 1619–1629. <https://doi.org/10.1145/3459637.3482264>
- [34] Jascha Sohl-Dickstein, Eric Weiss, Niru Maheswaranathan, and Surya Ganguli. 2015. Deep Unsupervised Learning Using Nonequilibrium Thermodynamics. In *Proceedings of the 32nd International Conference on Machine Learning*. PMLR, 2256–2265.
- [35] Jiaming Song, Chenlin Meng, and Stefano Ermon. 2020. Denoising Diffusion Implicit Models. In *International Conference on Learning Representations*.
- [36] Yusuke Tashiro, Jiaming Song, Yang Song, and Stefano Ermon. 2021. CSDI: Conditional Score-based Diffusion Models for Probabilistic Time Series Imputation. In *Advances in Neural Information Processing Systems*, Vol. 34. Curran Associates, Inc., 24804–24816.
- [37] Joojo Walker, Ting Zhong, Fengli Zhang, Qiang Gao, and Fan Zhou. 2022. Recommendation via Collaborative Diffusion Generative Model. In *Knowledge Science, Engineering and Management*, Gerard Memmi, Baijian Yang, Linghe Kong, Tianwei Zhang, and Meikang Qiu (Eds.). Springer International Publishing, Cham, 593–605. https://doi.org/10.1007/978-3-031-10989-8_47
- [38] Chao Wang, Hengshu Zhu, Qiming Hao, Keli Xiao, and Hui Xiong. 2021. Variable Interval Time Sequence Modeling for Career Trajectory Prediction: Deep Collaborative Perspective. In *Proceedings of the Web Conference 2021 (WWW '21)*. Association for Computing Machinery, New York, NY, USA, 612–623. <https://doi.org/10.1145/3442381.3449959>
- [39] Chao Wang, Hengshu Zhu, Peng Wang, Chen Zhu, Xi Zhang, Enhong Chen, and Hui Xiong. 2021. Personalized and Explainable Employee Training Course Recommendations: A Bayesian Variational Approach. *ACM Transactions on Information Systems* 40, 4 (Dec. 2021), 70:1–70:32. <https://doi.org/10.1145/3490476>
- [40] Chao Wang, Hengshu Zhu, Chen Zhu, Chuan Qin, Enhong Chen, and Hui Xiong. 2023. SetRank: A Setwise Bayesian Approach for Collaborative Ranking in Recommender System. *ACM Transactions on Information Systems* 42, 2 (Nov. 2023), 56:1–56:32. <https://doi.org/10.1145/3626194>

- [41] Hongwei Wang, Jia Wang, Jialin Wang, Miao Zhao, Weinan Zhang, Fuzheng Zhang, Xing Xie, and Minyi Guo. 2018. GraphGAN: Graph Representation Learning With Generative Adversarial Nets. *Proceedings of the AAAI Conference on Artificial Intelligence* 32, 1 (April 2018). <https://doi.org/10.1609/aaai.v32i1.11872>
- [42] Jun Wang, Lantao Yu, Weinan Zhang, Yu Gong, Yinghui Xu, Benyou Wang, Peng Zhang, and Dell Zhang. 2017. IRGAN: A Minimax Game for Unifying Generative and Discriminative Information Retrieval Models. In *Proceedings of the 40th International ACM SIGIR Conference on Research and Development in Information Retrieval (SIGIR '17)*. Association for Computing Machinery, New York, NY, USA, 515–524. <https://doi.org/10.1145/3077136.3080786>
- [43] Wenjie Wang, Yiyang Xu, Fuli Feng, Xinyu Lin, Xiangnan He, and Tat-Seng Chua. 2023. Diffusion Recommender Model. In *Proceedings of the 46th International ACM SIGIR Conference on Research and Development in Information Retrieval (SIGIR '23)*. Association for Computing Machinery, New York, NY, USA, 832–841. <https://doi.org/10.1145/3539618.3591663>
- [44] Xiang Wang, Xiangnan He, Meng Wang, Fuli Feng, and Tat-Seng Chua. 2019. Neural Graph Collaborative Filtering. In *Proceedings of the 42nd International ACM SIGIR Conference on Research and Development in Information Retrieval (SIGIR '19)*. Association for Computing Machinery, New York, NY, USA, 165–174. <https://doi.org/10.1145/3331184.3331267>
- [45] Yu Wang, Zhiwei Liu, Liangwei Yang, and Philip S. Yu. 2023. Conditional Denoising Diffusion for Sequential Recommendation. <https://doi.org/10.48550/arXiv.2304.11433> arXiv:2304.11433 [cs]
- [46] Yao Wu, Christopher DuBois, Alice X. Zheng, and Martin Ester. 2016. Collaborative Denoising Auto-Encoders for Top-N Recommender Systems. In *Proceedings of the Ninth ACM International Conference on Web Search and Data Mining (WSDM '16)*. Association for Computing Machinery, New York, NY, USA, 153–162. <https://doi.org/10.1145/2835776.2835837>
- [47] Zhengyi Yang, Jiancan Wu, Zhicai Wang, Xiang Wang, Yancheng Yuan, and Xiangnan He. 2023. Generate What You Prefer: Reshaping Sequential Recommendation via Guided Diffusion. In *Thirty-Seventh Conference on Neural Information Processing Systems*.